

IN SITU INVESTIGATION OF ELECTROCHEMICAL SURFACE STRESS  
DEVELOPMENT IN RECHARGEABLE BATTERIES

BY

YEONG-HUI SEO

THESIS

Submitted in partial fulfillment of the requirements  
for the degree of Master of Science in Chemistry  
in the Graduate College of the  
University of Illinois at Urbana-Champaign, 2018

Urbana, Illinois

Adviser:

Professor Andrew A. Gewirth

## ABSTRACT

Rechargeable batteries are everywhere these days such as portable electric devices and electric vehicles. The global annual sales of electric vehicles are increasing, showing the rechargeable battery market is obviously getting bigger. Li-ion batteries are operated by an intercalation mechanism. Lithium ions shuttle reversibly between the cathode and anode during charging and discharging. Typically, intercalation cathodes deliver around one hundred to two hundred in specific capacity. The operating voltage is around three to five vs. lithium. The current inorganic-compound cathodes have several challenges such as limited reserves and harmfulness to the environment due to the toxic materials released from current inorganic complexes. In contrast to the harmful current cathodes, organic cathode materials enable access to metal-free, environmentally benign rechargeable energy systems. Poly (1,4-anthraquinone) (PAQ) was chosen as the cathode material for this research based on its high capacity and super-stable cycle life. The reduction occurs as two reversible, continuous single-electron steps. PAQ was applied to the cathode vs. lithium and sodium. There are two types of stress evolutions arising from lithiation/sodiation and delithiation/desodiation. Accommodating metal ion process makes compressive stress whereas stripping metal ion process makes tensile stress. These two types of stress evolution was measured by employing in situ electrochemical stress measurement. Through the measurement, electrochemical property was analyzed thoroughly parallel with the change of stress and stress derivative. Obviously different behaviors of PAQ-composite cathode depend on lithium and sodium were analyzed.

## ACKNOWLEDGEMENTS

This work was supported by the Center for Electrochemical Energy Science, an Energy Frontier Research Center funded by the US Department of Energy, Office of Science, Basic Energy Sciences. I specially thank my supervisor, Andrew A. Gewirth to give an opportunity of joining his group, and doing this research. I still remember the first day I met Prof. Gewirth before transferring from MatSE to his group. I appreciate him for believing my potential and finally giving me the last chance of my research life. Support of synthesizing PAQ by Dr. Aaron Petronico is gratefully acknowledged. He was my mother duck, when I just joined Gewirth group. I never make this result without dedicated discussion and help of Kimberly, Bruno, and Minjeong. Prof. Hadi and Dr. Elizabeth helped for the discussion. I thank IMP office and Connie for administrative process. My case was unique and unprecedented, which administrative process is very complex. Connie has always helped me with kind smile, even after I came back to South Korea. Lastly, I thank the Department of Chemistry of our school. I thank god to allow me the time in Gewirth group. It was very short less than one year, but I hope this time would make my life more meaningful.

## TABLE OF CONTENTS

CHAPTER 1: INTRODUCTION .....	1
CHAPTER 2: EXPERIMENTAL .....	4
CHAPTER 3: ELECTROCHEMICAL SURFACE STRESS OF POLY (1,4- ANTHRAQUINONE) CATHODE IN LITHIUM AND SODIUM ION BATTERIES .....	6
REFERENCES .....	18

## CHAPTER 1: INTRODUCTION

Rechargeable batteries are everywhere these days such as portable devices and electric vehicles. The global annual sales of electric vehicles are increasing, showing the rechargeable battery market is obviously getting bigger.<sup>1</sup>

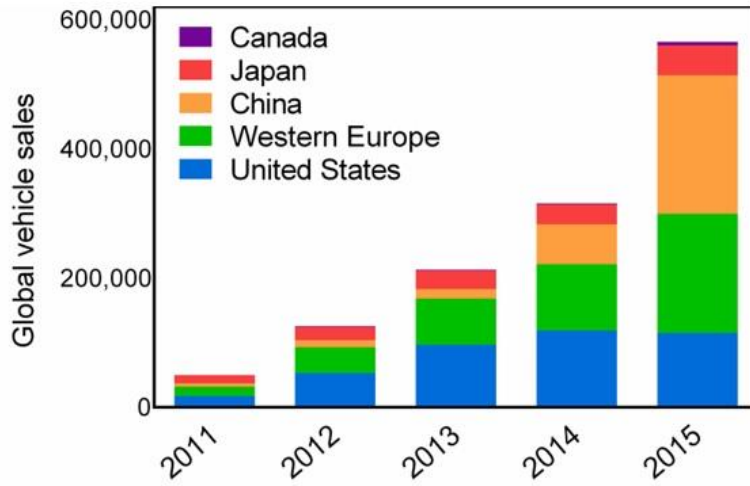


Figure 1. Worldwide Annual Sales of Electric Vehicles.<sup>1</sup>

People want to drive electric vehicles, with advantages such as no more consumption of coal or gasoline, high energy efficiency and fewer vehicle malfunctions. Li-ion batteries are operated by an intercalation mechanism. During charging and discharging, lithium ions shuttle reversibly between the cathode and anode.<sup>2</sup>

Typically, intercalation cathodes deliver around one hundred to two hundred in specific capacity. The operating voltage is around three to five vs. lithium.<sup>3</sup> The current inorganic-compound cathodes have several challenges. Their reserves are limited,<sup>4</sup> and they are harmful to the environment. The extraction of current inorganic complexes can release toxic materials. In addition, the synthesis procedure can create heavy-metal wastes.<sup>5-6</sup>

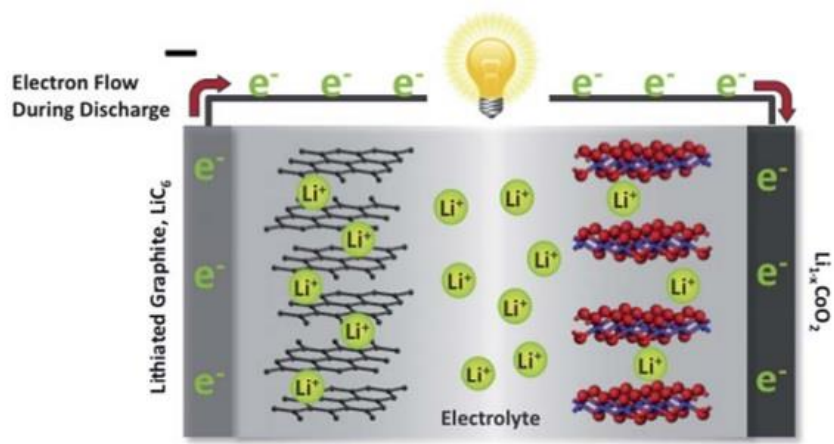
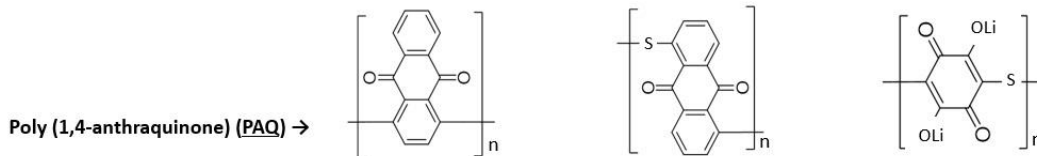


Figure 2. Intercalation Mechanism of Li-ion Batteries.<sup>2</sup>

In contrast to the harmful current cathodes, organic cathode materials enable access to metal-free, environmentally benign rechargeable energy systems. Therefore, their redox properties can be tailored by adjusting their molecular structure. Plus, they are composed of naturally abundant chemical elements.<sup>7</sup> After early 2010, carbonyl-based compounds with specific capacities higher than 200 mAh/g were reported, and greener cathode production with high performance seemed to be possible. Carbonyl-based organic compounds could provide capacities of up to 580 mAh/g. However, they suffered from dissolution in common electrolytes, leading to capacity fade.<sup>8-9</sup> The answer was to develop inherently insoluble compounds containing dense quinone groups to simultaneously satisfy the requirements for energy density and cycling stability. The structural variety of conjugated quinone compounds enabled a large potential window.<sup>7,10-11</sup> Poly (1,4-anthraquinone) (PAQ) was chosen as the cathode material for my research based on its high capacity and super-stable cycle life. The reduction occurs as two reversible, continuous single-electron steps, generating first the radical anion and then the dianion accompanying Li<sup>+</sup> association. In the re-oxidation process, carbonyl groups are rebuilt, and Li<sup>+</sup> is re-ejected into the electrolyte.



Reversible Capacity (mAh/g)	260	198	268
Voltage (V vs. Li/Li <sup>+</sup> )	2.14	2.2	2.03
Capacity Retention (%) [Cycle Number]	99.4 [1000]	90 [200]	90 [1500]

Figure 3. Candidates of Anthraquinone-based Polymer with High Capacity and Stable Cycle Life.<sup>7,10-11</sup>

PAQ was employed as cathode material vs lithium and sodium ion batteries. Both elements have a one-electron redox reaction at low potential, thus serving as the anode. Sodium resources are inexhaustible, and cheaper than lithium, so it would be greatly beneficial for large scale electric storage applications if sodium batteries could be built from organic materials. The current maximum energy density using an anthraquinone-based polymer cathode is 734 in a Li battery, and 557 Wh/kg in a Na battery, which are quite high values compared to conventional inorganic cathodes.<sup>10,12-15</sup> The electrochemical performance of anthraquinone-based cathode materials depends significantly on the substitution positions, binders, and electrolyte formulations. Materials with less steric hindrance at substitution positions show higher capacity and a longer cycle life.

In this paper, PAQ was applied to the cathode vs lithium and sodium. Both elements have a one-electron redox reaction at low potential, thus serving as the anode. The advantages of Na Compared to Li is that it is abundant and much cheaper, so it would be greatly beneficial for large scale electric storage applications if sodium batteries could be built from organic materials.

## CHAPTER 2: EXPERIMENTAL

In this research, Poly (1,4-anthraquinone) (PAQ) composite serves as a working electrode. Lithium and sodium metals serve as a Counter/Reference electrode. 1 M of bis(trifluoromethane)sulfonimide lithium in a mixture of 2:1 of 1,3-dioxolane:1,2-dimethoxyethane (v/v) was used as the electrolyte.

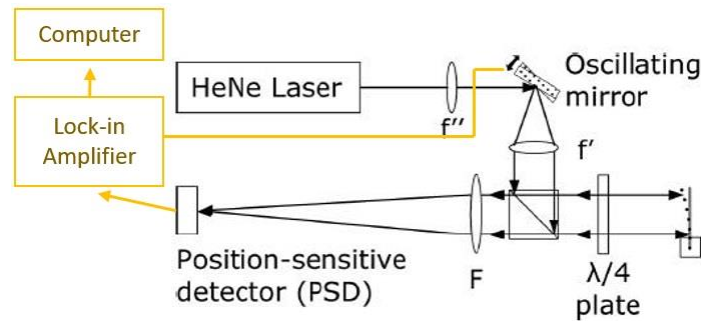


Figure 4. Optical Stress Measurement Setup.<sup>22-24</sup>

Researchers tried to optimize either the binders or electrolytes to achieve high energy density, testing the results with Cyclic Voltammetry (CV) and galvanostat cycling data.<sup>16-20</sup> Their results were limited. The authors figured out that something was causing higher or lower capacities, but they were not curious enough to pursue it more deeply.

There have been previous studies measuring in-situ stress evolution in Li-ion battery. During the lithium exchange process, structural and volume changes of the host materials contribute to changes in stress. Therefore, the surface-stress measurements provide important new insights into changes occurring at the host electrode during metal exchanges not discovered by other groups.<sup>21</sup> The optical setup employs a HeNe laser. A laser beam strikes the center of an oscillating mirror, and hits the cantilever passing through a beam splitter. The detector read the reflected laser. The detector is connected to the Lock-in amplifier, and it reads the laser at the set frequency only. Therefore, noise signals except the set frequency are rejected, then lock-in

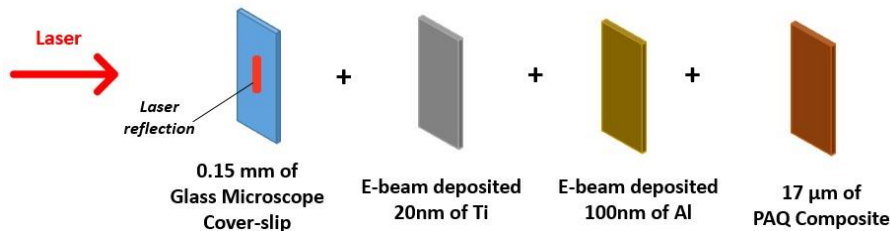


Figure 5. A Cutaway View of Coated Cantilever Beam.

amplifier send the filtered signals to the computer. The set frequency between the oscillating mirror and the lock-in amplifier must match to remove noises from any light sources in the laser room. The purpose of using lock-in amplifier with oscillating mirror is to maximize the signal to noise ratio. Stress changes can be calculated through Stoney's equation. Stress changes depend on the radius of curvature which depends on the voltage output. Stress evolution is related to the physical properties of a cantilever, such as the Elastic modulus and Poisson's ratio, and equipment properties such as primary lens focal length and the calibration constant of detector. The stress magnitude depends on the radius of curvature, which depends on the voltage output from the lock-in amplifier.<sup>22-24</sup>

PAQ composite was coated on the glass microscope cover-slip which is coated with titanium and aluminum shown in Figure 5. For measuring stress, a custom cell was used shown in Figure 6. The quartz window enables optical access of the laser.

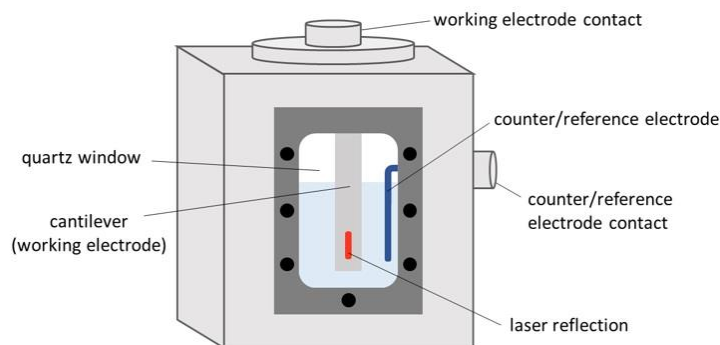


Figure 6. Custom Battery Cell for In Situ Stress Measurement.

### CHAPTER 3: ELECTROCHEMICAL SURFACE STRESS OF POLY (1,4-ANTHRAQUINONE) CATHODE IN LITHIUM AND SODIUM ION BATTERIES

Through this research, the electrochemical property and electrochemical surface stress of a poly (1,4-anthraquinone) (PAQ) cathode in lithium and sodium ion batteries was observed. In Figure 7, the cyclic voltammetry (CV) curve shows redox peaks centering at 2.2 and 1.7 V for lithium (Li) and sodium (Na), respectively. Both systems are electrochemically irreversible, which is consistent with the previous reports. For graph (b), the curves become broader and split and noisy on the anodic side. The interesting thing is that it has been observed consistently through three different potentiostat instruments. This needs to be figured out where that is coming from through employing different contacts in the cell configuration. If this noise would consistently exist, then it could be an electrolyte or other issues.

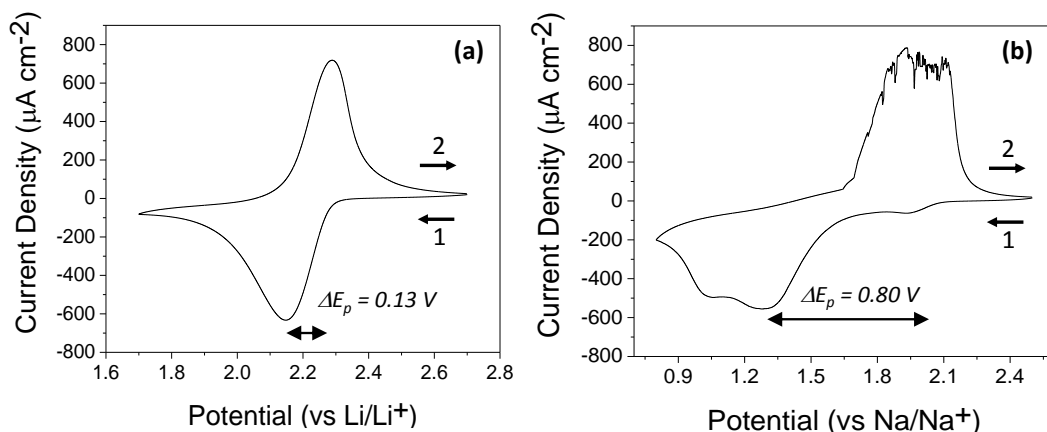


Figure 7. (a) CV Curve of PAQ Composite in 1 M Bis(trifluoromethane)sulfonimide Lithium (LiTFSI) in 2:1 of 1,3-dioxolane (DOL): 1,2-dimethoxyethane (DME) Electrolyte vs Li/Li<sup>+</sup>, (b) CV Curve of PAQ Composite in 1 M Bis(trifluoromethane)sulfonimide Sodium (NaTFSI) in 2:1 of DOL:DME Electrolyte vs Na/Na<sup>+</sup>.

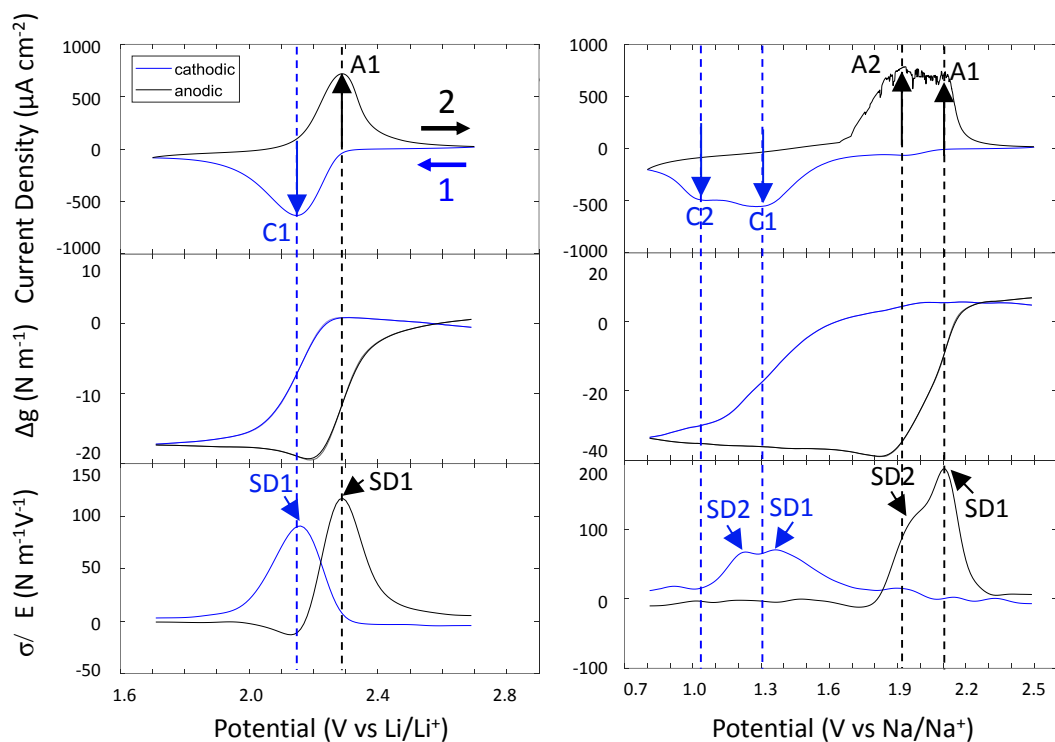


Figure 8. Potential-dependent Mechanical Response of PAQ Electrode vs (a)  $\text{Li/Li}^+$ , and (b)  $\text{Na/Na}^+$  at 1 mV/s.

The stress-measurement features (Figure 8) of Li and Na are quite different. In contrast to the different CVs, compressive stress developed by plating cations for both, and tensile stress developed by stripping cations. The stress derivative shows the rate of change. In the graph of the delta stress, the only thing to see is that compressive or tensile stresses are occurring. Plus, the stress derivative tells the potential where most actual stress changes are taking place. The abbreviations of C and SD mean the cathode and stress derivative, respectively. The number next to the word indicates the order of the redox pair. In Figure 8 (a), C1 and A1 are almost aligned with the cathodic and anodic SD1. However, SD1 comes up slightly earlier than C1, and SD2 comes up way earlier than C2 (Figure 8 (b)). We can't figure out the anodic peaks clearly because of the noise, but they seem to match pretty well.

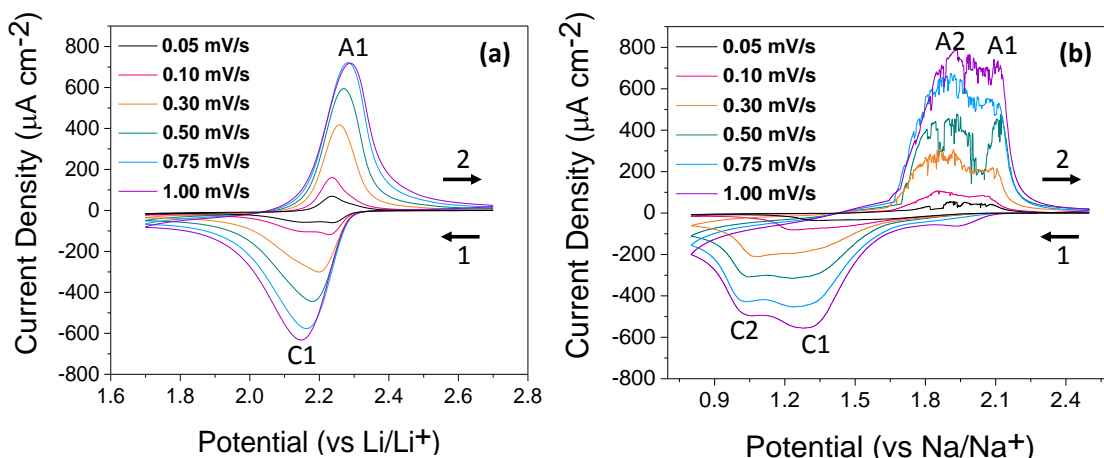


Figure 9. Scan Rate-dependent CV of PAQ Electrode in 1 M LiTFSI in 2:1 DOL: DME Electrolyte vs (a) Li/Li<sup>+</sup>, and Na/Na<sup>+</sup>.

The same experiments were performed with different scan rates from faster to slower. In Figure 9 (a), as the scan rate is getting slower, peak splitting starts to be observed. But in the Na case, the graphs always split into two cathodic peaks; C1, C2, A1, and A2 are merging as the scan rate slows down. The simple feature in the Li case is one pair of redox peaks, and the Na case has two pairs of redox peaks, caused by employing a different cation. It could be hard to plate and strip larger sodium cations. However, these interesting scan rate-dependent behaviors of splitting and merging peaks seem to come from the behavior of the polymer, not the cation. In the Li case, it could be that giving more time makes the polymer split the CV peak for some reason. In contrast, in the Na case, giving more time makes the polymer merge the CV peaks. In Figure 9 (b), the peak splitting kicks in at the slower scan rate. At a faster scan rate (Figure 10 (a)), the potential at the anodic peak current matches the potential at the peak stress derivative, whereas there is a slight pre-stress derivative peak compared to the cathodic peak current. However, at the slower scan rate in Figure 10 (b), there is the only one stress derivative peak, although there are two cathodic current peaks. It exists somewhere in the middle of the two

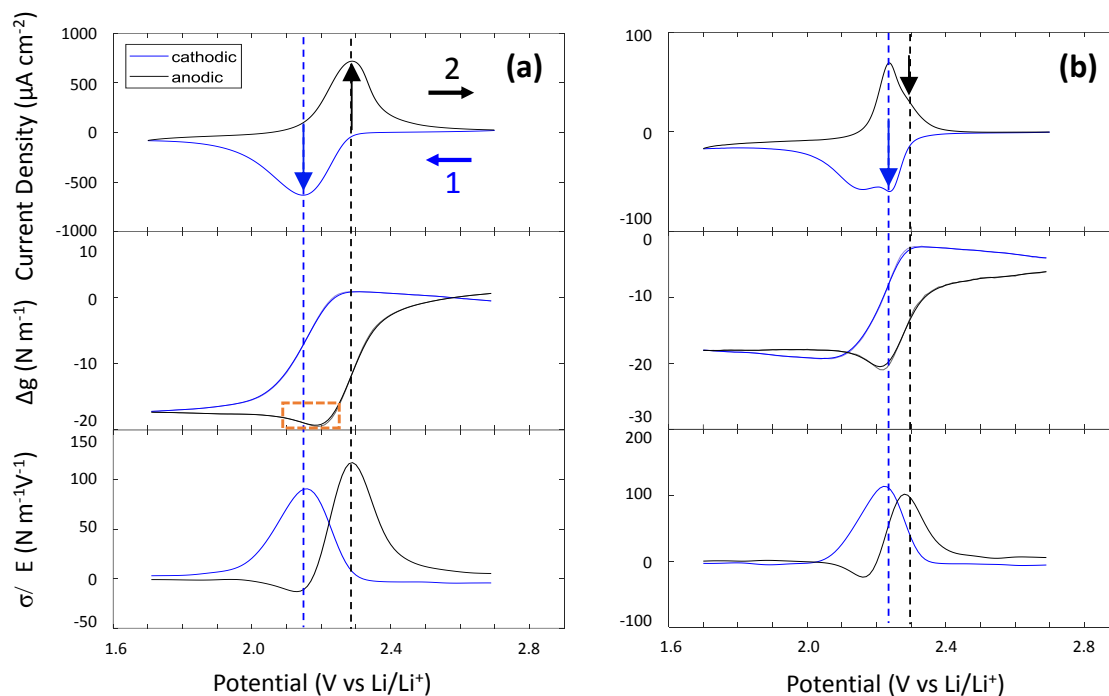


Figure 10.  $\Delta$ Stress and Stress Derivatives with Respect to Potential for CV vs Li/Li<sup>+</sup>

at (a) 1.0, and (b) 0.05 mV/s of Scan Rate.

cathodic current peaks. These arrows are pointing out the first pair of the redox reaction. There is a dip in the orange-dash box, and it gets deeper at the slower scan rate. In addition, irreversible stress developed at the slower scan rate.

There are three possible theory making these different features. The simplest part is a size difference. Larger Na cation has lower level of charge over size. In other words, effective positive charge of Li ion is bigger than Na ion. And Li ion is smaller, so accommodating Li ion could be easier than Na ion. Sodium ion is bigger, however, it has lesser effective charge. Therefore, accommodating Na ion in quinone group could be harder than Li ion. Second, there could be steric repulsion at the second step of sodiation due to the larger size. The last hypothesis could be related to the conformational changes of polymer. Xu et al. studied the similar quinone-based polymers having different conformations by changing the substitution position.

Interestingly, they reported that quinone-based polymer having more steric hinderance around carbonyl oxygen showed poor battery performance.<sup>19</sup> These results inspired this research that the conformation changes in polymer could affect the electrochemical and chemomechanical behaviors. For checking possibility of conformational changes, simple energy minimization of lithiated and sodiated PAQ using Chem Draw program was run. Because MM2 method can be used to predict the energy of large molecules as a function of its conformation. It was demonstrated that PAQ itself has staggered conformation. The staggered PAQ started to gather accommodating cations. It's not clear if PAQ would be much deformed by accommodating sodium than lithium or not. However, the possibility of the conformational changes of PAQ was confirmed by this simple tool. More professional tool needs to be applied to calculate the minimum energy configuration of polymer.

There is compressive stress development by lithiation and tensile stress development by delithiation. However, just before delithiation, an unexpected dip and the magnitude of the dip were observed. Another stress feature is an irreversible delta stress after one full cycle, and the represents the magnitude of stress that failed to recover. These two stress changes obviously

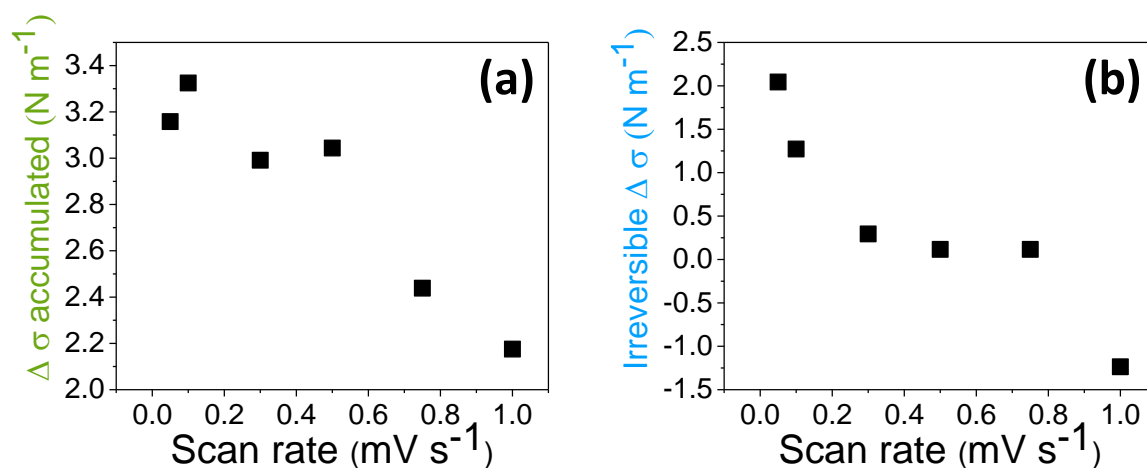
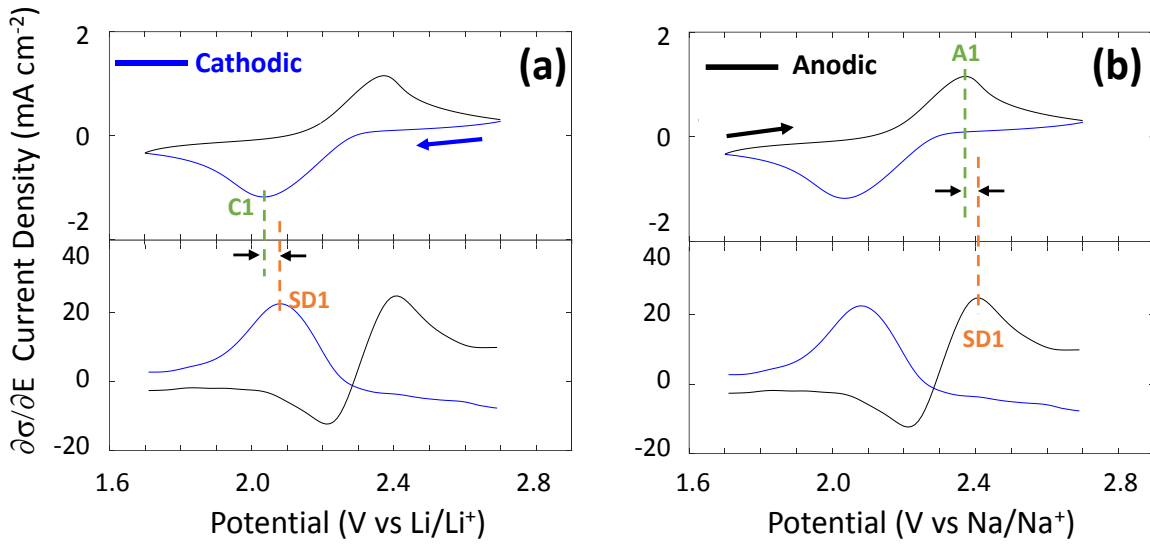


Figure 11. ΔStress Accumulated and Irreversible ΔStress with Different Scan Rates vs Li/Li<sup>+</sup>.



**Cathodic**  
Larger " $V_{\max. \partial\sigma/\partial E} - V_{\max. J_s} (V)$ " = PRE-stress

**Anodic**  
Larger " $V_{\max. \partial\sigma/\partial E} - V_{\max. J_s} (V)$ " = POST-stress

Figure 12. Deviation Magnitude of Potentials between CV and  $\partial\sigma/\partial E$ , (a) Pre-stress, and

(b) Post-stress.

exist as a function of scan rate. Stress accumulated and irreversible stress are getting increased at slower scan rate. As the scan rate goes slow, polymer could have more time to deform accommodating lithium ions. When the lithium ions are removed from PAQ, there could a balancing of accumulated residual stress generating this dip. More accumulating stress could make this inelastic deformation.

There are two concepts of pre-stress and post-stress derivative peaks compared to CV peaks. From cathodic side shown in Figure 12 (a), the potential mismatch can be calculated by subtracting C1 potential from SD1 potential. Larger difference means there is pre-stress before reduction. From anodic side shown in Figure 12 (b), the potential mismatch can be calculated by subtracting A1 potential from SD1 potential. Larger difference means there is post-stress after oxidation. Therefore, the deviation can tell the presence of pre- or post-stress development.

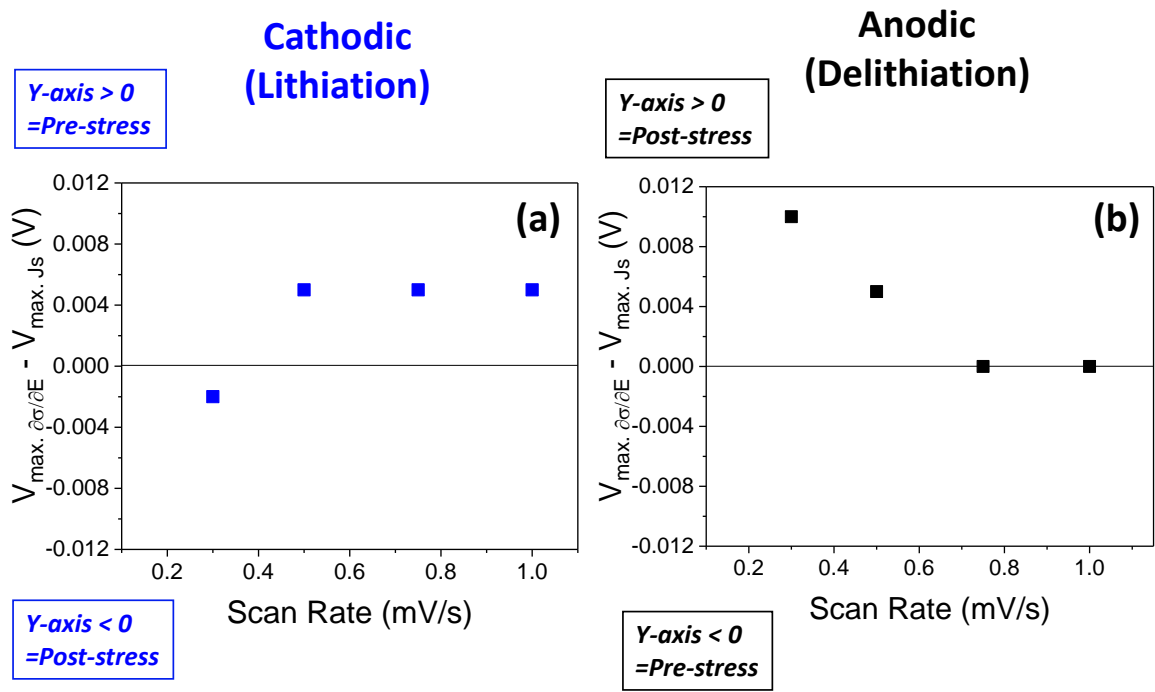


Figure 13. Deviation Magnitude of Potentials between CV and  $\partial\sigma/\partial E$  vs  $\text{Li}/\text{Li}^+$  (a) Cathodic Side, and (b) Anodic Side.

At the cathodic side vs  $\text{Li}/\text{Li}^+$  shown in Figure 13 (a), the post-stress development was observed at slower scan rate. The tendency could be in the error range and there could be flat pre-stress developments regardless of scan rate. However, the increase of post-stress development was clearly observed during delithiation. Therefore, there could be more stress after delithiation detangling the structure, because polymer could be more deformed accommodating lithium ions at slower scan rate. At a slower scan rate in the result of scan rate dependent mechanical response vs  $\text{Na}/\text{Na}^+$  shown in Figure 14, C1 is disappearing, shifting SD1 to more right. Interestingly, there are no irreversible stress which is opposite behavior in Li case. This tendency is because accommodating Na ions is easy due to the lower effective charge. Large size of Na ions produce lower effective charge, and it makes Na ions leave the carbonyl oxygen easily. Therefore, there could be no irreversible stress.

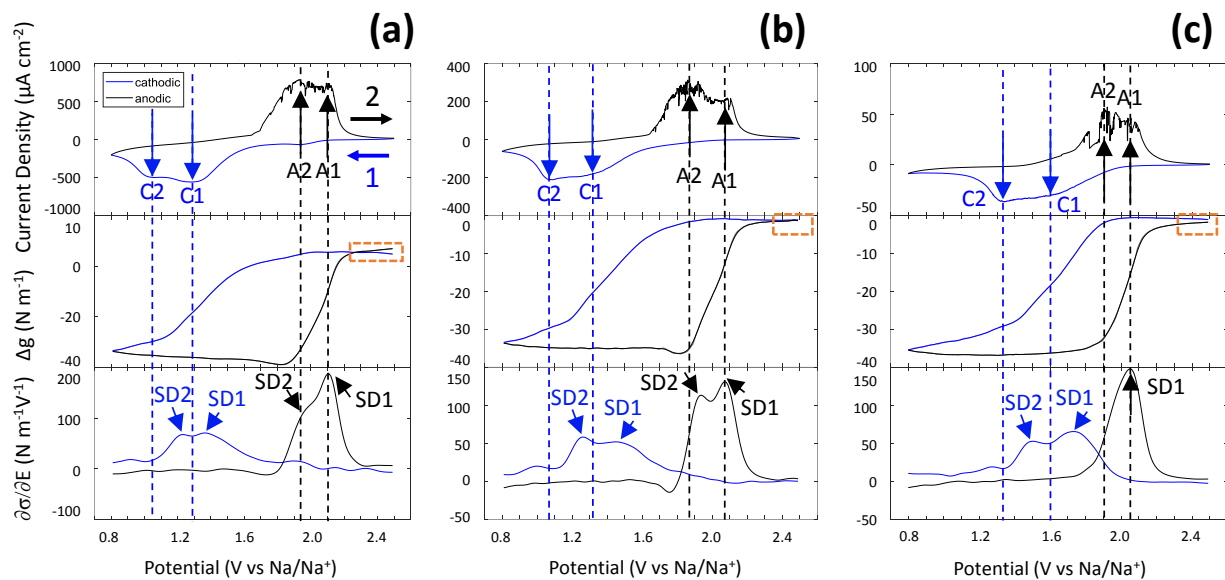


Figure 14. Potential-dependent Mechanical Response of PAQ Electrode vs  $\text{Na}/\text{Na}^+$  at (a) 1 mV/s, (b) 0.3 mV/s, and (c) 0.05 mV/s of Scan Rate.

As explained in Li case before, scan rate dependent accumulated stress was observed shown in Figure 15. The unexpected dip before desodiation was also observed. Accumulated stress is getting decreased at slower scan rate which is opposite behavior to Li case. Lithiation and delithiation behave quite different compared with sodiation and desodiation. Higher accumulated stress at this point could be caused by faster accommodation of large sodium ions. Therefore, there could be lesser stress because there is enough time for sodiation at slower scan rate.

The presence of pre- or post-stress in Na case was compared to Li case shown in Figure 16. The centers of two cathodic peaks, A1, and SD1 peaks were considered for the calculations. The exact calculations are arguable in this research, however it is obvious that there is a tendency. At the cathodic side, the pre-stress development could be observed at slower scan rate, whereas there is not much difference at anodic side. The pre-stress development at faster scan rate could be caused by diffusion of large Na ions. The increase of pre-stress development at faster scan

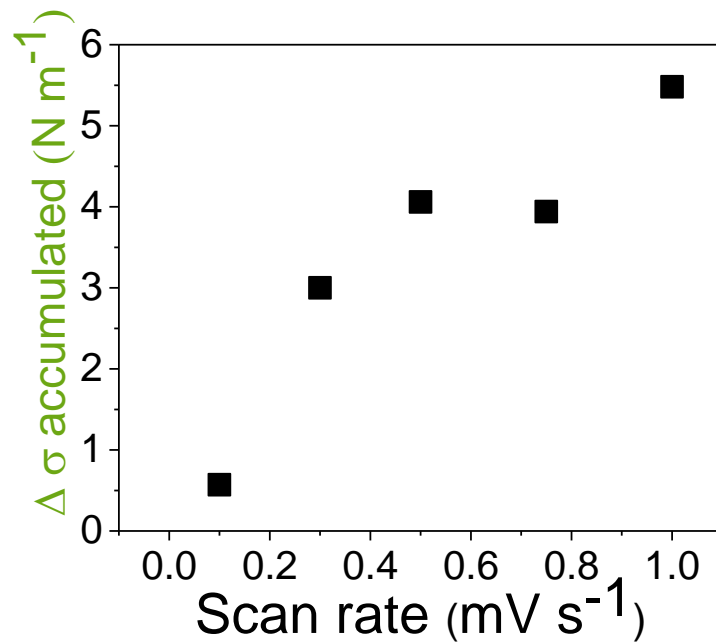


Figure 15.  $\Delta\sigma$  Accumulated with Different Scan Rates vs Na/Na<sup>+</sup>.

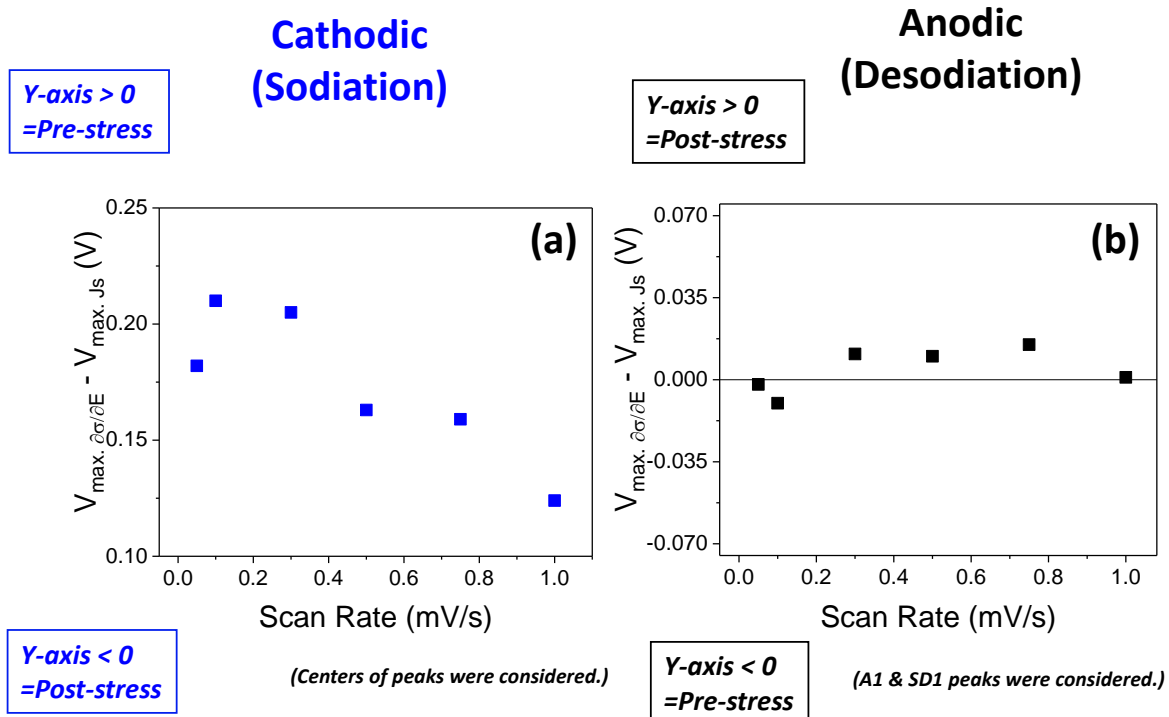


Figure 16. Deviation Magnitude of Potentials between CV and  $\partial\sigma/\partial E$  vs Na/Na<sup>+</sup> (a) Cathodic Side, and (b) Anodic Side.

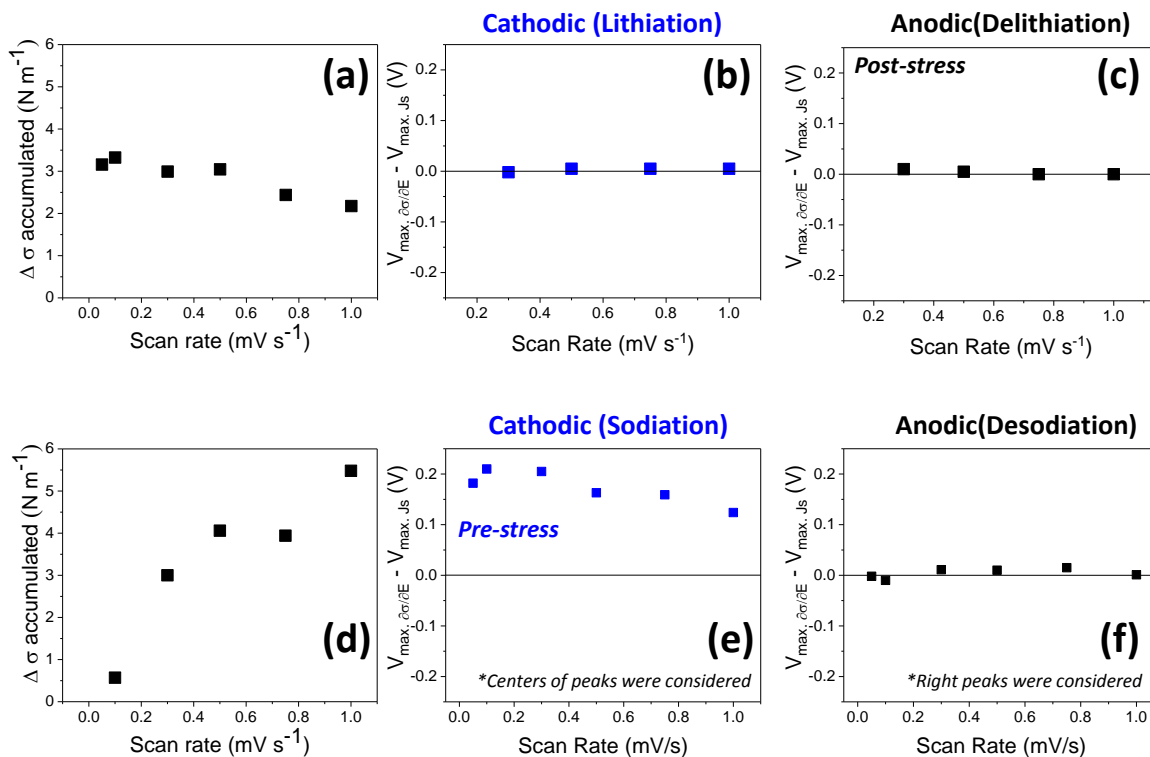


Figure 17. (a)  $\Delta$ Stress accumulated, deviation magnitude of potentials between CV and  $\partial\sigma/\partial E$  at (b) cathodic side, and (c) anodic side vs  $\text{Li}/\text{Li}^+$ , (d)  $\Delta$ Stress accumulated, deviation magnitude of potentials between CV and  $\partial\sigma/\partial E$  at (e) cathodic side, and (f) anodic side vs  $\text{Na}/\text{Na}^+$ .

rate could be lesser effective charge. To accommodate large Na ions, the conformation changes could be required. For desodiation process, Na ions could be leave from polymer easily due to their lesser effective charge.

In conclusion, as shown in Figures 17 (a) and 17 (c),  $\Delta$ stress accumulated, and post-stress development increases as the scan rate goes down. It could be caused by the accumulated stress from the history-dependent cycling and the solid-electrolyte interphase formation. There could be pre- or post- stress derivative peaks compared to CV peaks. From the cathodic side, this mismatch of potential can be calculated by subtracting the C1 potential from the SD1 potential. A larger difference means the existence of pre-stress before reduction of the active materials. On

the anodic side, this mismatch of potential can be calculated by subtracting the A1 potential from the SD1 potential. A larger difference means the existence of post-stress after oxidation of the active materials. Therefore, these deviations in Figure 17 (b) and 17 (c) can tell the presence of pre- or post- stress development. On the cathodic side (Figure 17 (b)), post-stress development could be observed as the scan rate slowed down; or this point could be in the error range, and there could be flat pre-stress developments regardless of the scan rate. However, the increase of post-stress development was clearly observed on the anodic side (Figure 17 (c)). Compared to the tendency of lithiation and delithiation, the different behavior of PAQ vs Na/Na<sup>+</sup> was summarized shown in Figure 17 (d), Figure 17 (e), and Figure 17 (f). For direct comparison, all of these are plotted on the same scale. There is obvious difference between lithiation/delithiation and sodiation/desodiation. There are bigger accumulated stress with sodium ions at faster scan rate, and it decreases dramatically at slower scan rate. Lithiation and delithiation process show the opposite behavior with much smaller magnitude. In addition, from these plots, there are increasing pre-stress development before sodiation and increasing post-stress development before lithiation. Therefore, it is likely that Li ions easily come in due to the smaller size and higher effective charge, but hard to come out due to the higher effective charge. In contrast, sodium ions hard to come in due to the larger size and lesser effective charge, but easily to come out due to the lesser effective charge.

There are hypotheses made based on the stress data, which need to be demonstrated. There is a couple of different techniques to solve these issues: 2-dimensional nuclear magnetic resonance and circular dichroism. These analyses will enable to observe a cation-plated structure compared to its pristine status. Another research that can be done is to find the right group and talk to them about a simulation to confirm the changes to PAQ by plating or stripping metal

cations. The density-functional theory, which is a computational quantum-mechanical modeling method for investigating electronic structures, could be the proper tool for the simulation. If this research would be successfully done, then electrochemical surface stress of PAQ cathode in multivalent ion batteries would be deeper project in future. The current research would be extended the same PAQ cathode to multivalent ions such as zinc or aluminum. This research expects to prove that PAQ's redox behavior could be different depending on whether it uses monovalent or multivalent cations through measuring electrochemical surface stress.

## REFERENCES

1. Global Annual Sales of Electric Vehicles data compiled by Argonne National Laboratory.
2. Thackeray, M. M.; Wolvertonb, C.; Isaacs, E. D. Electrical energy storage for transportation-approaching the limits of, and going beyond, lithium-ion batteries *Energy Environ. Sci.*, **2012**, 5, 7854-7863.
3. Nitta, N; Wu, F.; Lee, J. T.; Yushin, G. Li-ion battery materials: present and future *Materials Today* **2015**, 18, 5, 252-264.
4. Shao, M.; Chang, Q.; Dodelet, J.- P.; Chenitz, R. Recent Advances in Electrocatalysts for Oxygen Reduction Reaction *Chem. Rev.* **2016**, 116, 3594-3657.
5. Schon, T. B.; McAllister, B. T.; Li, P.- F.; Seferos, D. S. The rise of organic electrode materials for energy storage *Chem. Soc. Rev.*, **2016**, 45, 6345-6404.
6. Application of Life Cycle Assessment to Nanoscale Technology: Lithium-ion Batteries for Electric Vehicles **2013**.
- 7 Liang, Y.; Tao, Z.; Chen, J. Organic Electrode Materials for Rechargeable Lithium Batteries *Adv. Energy Mater.*, **2012**, 2, 742-769.
8. Zhu, Z.; Hong, M.; Guo, D.; Shi, J.; Tao, Z.; Chen, J. All-Solid-State Lithium Organic Battery with Composite Polymer Electrolyte and Pillar[5]quinone Cathode *J. Am. Chem. Soc.*, **2014**, 136, 47, 16461-16464.
9. Chen, H.; Armand, M.; Demailly, G.; Dolhem, F.; Poizot, P.; Tarascon, J.- M. From Biomass to a Renewable  $\text{Li}_x\text{C}_6\text{O}_6$  Organic Electrode for Sustainable Li-Ion Batteries *Chem Sus Chem* **2008**, 1, 348-355.

10. Haupler, B.; Wild, A.; Schubert, U. S. Carbonyls: Powerful Organic Materials for Secondary Batteries *Adv. Energy Mater.* **2015**, 5, 1402034, 1-34.
11. Song, Z.; Zhou, H. Towards sustainable and versatile energy storage devices: an overview of organic electrode materials *Energy Environ. Sci.*, **2013**, 6, 2280-2301.
12. Xu, F.; Xia, J.; Shi, W. Anthraquinone-based polyimide cathodes for sodium secondary batteries *Electrochemistry Communications* **2015**, 60, 117-120.
13. Slater, M. D.; Kim, D.; Lee, E.; Johnson, C. S. Sodium-Ion Batteries *Adv. Funct. Mater.* **2013**, 23, 947-958.
14. Song, Z.; Qian, Y.; Zhang, Tao.; Otani, M.; Zhou, H. Poly(benzoquinonyl sulfide) as a High-Energy Organic Cathode for Rechargeable Li and Na Batteries *Adv. Sci.* **2015**, 2, 1500124, 1-9.
15. Kim, S.- W.; Seo, D.- H.; Ma, X.; Ceder, G.; Kang, K. Electrode Materials for Rechargeable Sodium-Ion Batteries: Potential Alternatives to Current Lithium-Ion Batteries *Adv. Energy Mater.* **2012**, 2, 710-721.
16. Ding, Y.; Li, Y.; Yu, G. Exploring Bio-inspired Quinone-Based Organic Redox Flow Batteries: A Combined Experimental and Computational Study *Chem.* **2016**, 1, 790-801.
17. Xie, J.; Wang, Z.; Gu, P.; Zhao, Y. J.; Xu, Z.; Zhang Q. A novel quinone-based polymer electrode for high performance lithium-ion batteries *Science China Materials* **2016**, 59, 1, 6-11.
18. Song, Z.; Qian, Y.; Gordin, M. L.; Tang, D.; Xu, T.; Otani, M.; Zhan, H.; Zhou, H.; Wang, D. Polyanthraquinone as a Reliable Organic Electrode for Stable and Fast Lithium Storage *Angew. Chem. Int. Ed.* **2015**, 54, 1-6.
19. Xu, W.; Read, A.; Koech, P. K.; Hu, D.; Wang, C.; Xiao, J.; Padmaperuma, A. B.; Graff, G. L.; Liuc, J.; Zhang, J.- G. Factors affecting the battery performance of anthraquinone-based organic cathode materials *J. Mater. Chem.*, **2012**, 22, 4032-4039.

20. Song, Z.; Zhan, H.; Zhou, Y. Anthraquinone based polymer as high performance cathode material for rechargeable lithium batteriesw *Chem. Commun.*, **2009**, 448-450.
21. Tavassol, H.; Jones, E. M. C.; Sottos, N. R.; Gewirth, A. A. Electrochemical stiffness in lithium-ion batteries *Nature Materials* **2016**, 15, 1182-1187.
22. Langer, J. L.; Economy, J.; Cahill, D. G. Absorption of Water and Mechanical Stress in Immobilized Poly(vinylbenzyltrialkylammonium chloride) Thin Films *Macromolecules* **2012**, 45, 3205-3212.
23. Zhang, X.; Cahill, D. G. Measurements of Interface Stress of Silicon Dioxide in Contact with Water-Phenol Mixtures by Bending of Microcantilevers *Langmuir* **2006**, 22, 9062-9066.
24. Haiss, W. Surface stress of clean and adsorbate-covered solids *Rep. Prog. Phys.* **2001**, 64, 591-648.